

Upcycling of post-consumer PLA into active packaging films: Structural and functional assessment of rPLA/PCL blends with quercetin

Andrea Feroce^b, Sara Exojo-Trujillo^a, José Manuel López Vilariño^c, Fabio Licciardello^{b,d}, Rafael Gavara^a, Carol López-de-Dicastillo^{a,*}

^a Packaging Group, Institute of Agrochemistry and Food Technology (IATA-CSIC), Av. Agustín Escardino 7, Paterna 46980, Spain

^b Department of Life Sciences, University of Modena and Reggio Emilia, via Amendola 2, Reggio Emilia 42122, Italy

^c Hijos de Rivera SAU, José María Rivera Corral 6, A Coruña, Spain

^d Interdepartmental Research Centre for the Improvement of Agro-Food Biological Resources (BIOGEST-SITEIA), University of Modena and Reggio Emilia, Piazzale Europa 1, Reggio Emilia 42122, Italy

ARTICLE INFO

Keywords:

Recycling
Post-consumer
Poly(lactic acid)
Polycaprolactone
Quercetin
Active packaging

ABSTRACT

The detrimental impact on the environment derived from the wrong management of conventional plastics is promoting the use of biobased and biodegradable materials for food packaging. Specifically, poly(lactic acid) (PLA) is characterized by its compostability, availability and its easy processing by melt extrusion, becoming one of the most used biopolymers in the industry. Because PLA is a valuable polyester, its recyclability should be considered as an alternative to compostability. In this work, the post-consumer recycled PLA (rPLA) obtained after simulating the service life and recycling processes of commercial PLA-based water bottles was used to develop new active packaging systems. Polycaprolactone (PCL), a polyester known for its excellent deformability, was added to mitigate the deterioration of rPLA during its reprocessing and afford different characteristics. Likewise, the addition of quercetin (Q), a natural polyphenolic antioxidant, can increase the interaction between both polymers and allow a greater preservation of food sensitive to oxidation through its progressive release. In this work, active films based on rPLA and PCL blends at different ratios (85/15 and 70/30) incorporating Q at 3 wt% were melt-extruded. Thermal, optical, diffusional (specific and overall migration) and morphological properties were analyzed, in addition to their antioxidant capacity and Q release profiles. Micrographs showed polymeric blends exhibited spherical-shaped PCL particles surrounded by rPLA matrix, and their characterization indicated the blending with PCL and Q increased rPLA crystallinity. In addition, the release of Q and their antioxidant activity increased with PCL concentration and ethanol content in the food simulant.

1. Introduction

According to the United Nations Environment Programme (UNEP), plastics contribute to more than a third of the production in the packaging sector, such as bottles, containers, and grocery bags (Ncube et al., 2021). In addition, approximately 79 % of plastic waste is estimated to end up in landfills or natural environments (Geyer et al., 2017; Hahladakis et al., 2018). Given the problems linked to the accumulation of plastic waste and the difficulties on their collection and separation in the recycling centers, the interest towards the possibility to use biodegradable plastics from renewable sources is gaining popularity (Ncube et al., 2021). The European Union through its European Green Deal (EC-European Commission, 2019) and Circular Economy Action Plan (EC-

European Commission, 2020) has introduced a policy framework regarding bio-based, biodegradable and compostable plastics (EC-European Commission, 2022). Among these, bio-polyesters such as polylactic acid (PLA), polyhydroxyalkanoate (PHA), polyhydroxybutyrate (PHB), and polyhydroxybutyrate valerate (PHBV) have attracted growing interest in recent years (Shen et al., 2020). PLA is the most used for a number of advantages, including ease of processing, high transparency and inherent biodegradability. However, it also has disadvantages such as sensitivity to thermal degradation, poor barrier properties and brittleness (Agüero et al., 2023). Its waste management is not so immediate, specific conditions are required to biodegrade in specific environment, such as industrial compost at 58 °C, pH around 7.5, relative humidity of 60 %, C/N ratio between 20:1 and 40:1 and correct

* Corresponding author.

E-mail address: clopezdedicastillo@iata.csic.es (C. López-de-Dicastillo).

<https://doi.org/10.1016/j.fpsl.2026.101700>

Received 24 July 2025; Received in revised form 14 December 2025; Accepted 5 January 2026

2214-2894/© 2026 The Authors. Published by Elsevier Ltd. This is an open access article under the CC BY-NC license (<http://creativecommons.org/licenses/by-nc/4.0/>).

aeration (Arrieta, 2021). These factors significantly slow down the degradation of most PLA-based packaging. Other routes for PLA waste management could be energy recovery and chemical or mechanical recycling (Badia et al., 2017; Hahladakis et al., 2018). As previously mentioned, composting is a slow process that requires specific conditions, and many composting plants are still reluctant to accept this material. Energy recovery, on the other hand, involves the thermal breakdown of PLA to produce energy. However, neither method is advantageous, as neither allows for a reduction in the demand for producing new PLA (Badia et al., 2017; Casto-Aguirre et al., 2016). Chemical recycling consists in the depolymerization of PLA into its original monomers, which can then be used to produce new material. While promising in theory, the environmental and economic impact compared to other types of recycling and to sourcing virgin raw materials must be considered (Jannatiha & Gutiérrez, 2025; Soroudi & Jakubowicz, 2013). Meanwhile, mechanical recycling consists in the recovery, selection, grinding and reprocessing of PLA waste. Currently, it appears to be the revaluation and waste management method with the least environmental impact (Cosate de Andrade et al., 2016; Rossi et al., 2015).

The growing interest in promoting the use of sustainable alternative plastics has led a Spanish company to develop PLA-based water bottles. This study aims to assess the feasibility of using this post-consumer plastic waste as raw material for the development of active food packaging. First, the simulation of their service life and mechanical recycling processes were carried out in order to obtain the post-consumer recycled PLA (rPLA). This served as a starting point to study how this post-consumer packaging can be part of new active systems promoting a circular economy. This study was focused on the development of antioxidant packaging systems based on blends of rPLA-based bottles, polycaprolactone (PCL) and quercetin (Q), a natural antioxidant, as an active compound, and the research of the effect of incorporating rPLA and PCL on the physical properties and the release of the antioxidant compound. Quercetin is a flavonoid widely found in foods, known for its antioxidant and anti-inflammatory properties, as well as for its role in reducing mycotoxins and promoting cellular protection (Qi et al., 2022; Yang et al., 2020). It exerts antioxidant effects by scavenging reactive oxygen species (ROS) directly through its hydroxyl (-OH) groups, chelating metal ions such as iron and copper to prevent free radicals generation and ROS-generating reactions, modulating glutathione levels and the activity of antioxidant enzymes, and regulating signal transduction pathways involved in oxidative stress and inflammation (Jasrotia et al., 2025; Qi et al., 2022). On the other hand, PCL is a linear thermoplastic polyester, partially crystalline, biodegradable and with good extensibility, mechanical properties and barrier properties (Maurizzi et al., 2022). This polymer finds application in food packaging as biodegradable films and bags, and it is also investigated for its role in active food packaging as a carrier of active compounds (Thakur et al., 2021). Various studies have already reported that the blend between PCL and PLA improved the mechanical properties of PLA, reduced brittleness and slight increased its thermal stability (Thakur et al., 2021; Haq et al., 2017; Wachirahutpong et al., 2016; Jain et al., 2010; Kemala et al., 2012). Nevertheless, the development of active systems by using rPLA and PCL has not been carried out so far. Thus, the main goal of this investigation was studying the effect of developing an active system based on rPLA and the incorporation of PCL at two concentrations on the release of quercetin and its subsequent functionality, as well as, the effect on the physical properties of this recycled bioplastic based on rPLA.

The chemical, structural, optical and thermal properties of active rPLA-PCL blends were characterized, as well as their overall migration of compounds and the analysis of specific migration of quercetin, in addition to their antioxidant activities.

2. Materials and methods

2.1. Materials

Commercial green PLA (polylactic acid)-based water bottles (0.50 L size) were supplied by Cabreiroá (Hijos de Rivera S.A.). Sodium hydroxide (NaOH) was purchased from Fluka Biochemika (Barcelona, Spain). Triton™ X-100 surfactant, 2,2'-azinobis(3-ethylbenzothiazoline-6-sulphonate) (ABTS), potassium persulfate and tetrahydrofuran (THF) (99.9 %) were supplied by Sigma Aldrich (Madrid, Spain). Silica gel 2.5–6 mm with indicator (without cobalt chloride) was purchased from PanReac (Barcelona, Spain). Ultrapure water was obtained from a Milli-Q Plus purification system (Millipore, Molsheim, France).

2.2. Post-consumer recycling simulation

In order to obtain the post-consumer recycled PLA (rPLA), the commercial PLA-based water bottles were subjected to a prior accelerated ageing and recycling simulations following established protocols owing to simulate their degradation during service life and mechanical recycling processes (Arjona et al., 2026). According to the process followed by Beltrán et al. (2019), the commercial PLA bottles were photochemically degraded in a UV chamber equipped with eight F40UVB lamps for 40 h. Then, bottles were exposed to thermal degradation in a convection oven at 50 °C for 468 h, followed by a hydrothermal aging at 25 °C for 240 h in deionized water (Beltrán et al., 2019). Finally, the aged samples followed a washing process typically from secondary mechanical recycling plastics. Bottles were washed at 85 °C for 15 min in a solution of 1.0 wt% NaOH solution (and 0.3 wt% Triton X, as surfactant). Then the bottles were washed with distilled water and dried in an oven at 40 °C for 48 h. After these processes, the PLA bottles were mechanically ground at a size of 4 mm, resulting on post-consumer recycled rPLA sample.

2.3. Development of rPLA-PCL-Q blends

Recycled bottles were ground using a rotating steel blade in a SM 300 cutting mill (Retsch, Asturias, Spain) operating at 1800 rpm with a 4 mm diameter sieve. rPLA was dried in a vacuum oven at 40 °C for 16 h. As shown in Table 1, two PLA-PCL blends at 85–15 and 70–30 ratios were obtained. Active blends were processed by adding quercetin at 3 wt% respect to the total polymer weight. rPLA-PCL-Q blends and their corresponding controls were processed through melt extrusion in a MC 15 HT co-rotating twin-screw extruder (L/D = 30) (Xplore, Barcelona, Spain) at 180 °C from the feed hopper to the extrusion outlet. The extrusion process was conducted at a rotation speed of 100 rpm with a residence time of 3 min.

Samples obtained from mini-extruder were ground and thermo-compressed into films in order to characterize some properties. The hot plates were set at 180 °C with a pressure of 80 bar for 3 min, followed by 2 min of cooling. This process yielded films with an approximate thickness of 100 ± 20 µm.

Table 1
Composition and names of developed films.

Sample	Abbreviation
PLA from water bottle	PLA
recycled PLA	rPLA
85 %wt. rPLA + 15 %wt. PCL	85rPLA15PCL
70 %wt. rPLA + 30 %wt. PCL	70rPLA30PCL
PLA + 3 %wt. Q	PLA3Q
rPLA + 3 %wt. Q	rPLA3Q
85 % wt. rPLA + 15 %wt. PCL + 3 %wt. Q	85rPLA15PCL3Q
70 %wt. rPLA + 30 %wt. PCL + 3 %wt. Q	70rPLA30PCL3Q

2.4. Film characterization

2.4.1. Field emission scanning electron microscopy (FESEM) analysis

The morphology of the cross-section of the films was characterized using a field emission scanning electron microscope FESEM (SCIOS 2, Thermo Fisher Scientific, USA). Samples were first cryofractured to obtain a clean cross section that was coated with a gold-palladium alloy for 60 s. The test conditions for the acceleration voltage were 5 kV, 0.20 nA and 20000 × magnification. The diameter of PCL particles contained was measured using Image J software. The average diameter values of the PCL particles were calculated considering a representative image area of 610 μm².

2.4.2. Color

The color of developed films was evaluated using a CM 3500 colorimeter (Konica Minolta, Dietikon, Switzerland) with SpectraMagic NX software. The instrument was calibrated using a blank and the samples were measured with a standard cylindrical accessory for black (no light reflection). The measurement of grinded samples were taken in triplicate and results were expressed on the CIELab color scale by determining L*, a* and b* parameters that indicated the lightness, reddish/greenish and yellowish/bluish, respectively. For this purpose, an illuminant D65 and a standard observer of 10° were considered. Following Eq. 1 and comparing with the PLA₀ color coordinates, the color difference (ΔE*_{ab}) was calculated:

$$\Delta E_{ab}^* = \sqrt{(\Delta L^*)^2 + (\Delta a^*)^2 + (\Delta b^*)^2} \quad (1)$$

2.4.3. Thermal properties

The thermal degradation of films and their components were evaluated using a thermogravimetric analyzer TGA 5500 (TA Instruments, USA). The samples were heated from 20 to 800 °C at a heating rate of 20 °C min⁻¹ and nitrogen flow of 50 mL min⁻¹. The temperature of maximum degradation rate (T_{max}) was determined using the TRIOS software.

Films were also analyzed using differential scanning calorimetry (DSC) with Q2000 equipment (TA Instruments, USA) under nitrogen at a flow rate of 50 mL min⁻¹. Samples were conditioned in desiccators containing P₂O₅ at 25 °C until constant weight before the analysis. Approx. 10 mg of sample was weighted in alumina pans and submitted to a heating temperature ramp from -20–220 °C, followed by a cooling from 220 °C to -20 °C at 10 °C min⁻¹ with an isothermal equilibration of 2 min at each temperature change. The values of glass transition temperature (T_g), maximum melting temperature (T_m), cold crystallization temperature (T_{cc}) and their corresponding enthalpies were calculated using TA Instruments Universal Analysis 2000 software by analyzing the thermograms corresponding to the second heating process. The crystallinity (χ_c) of PLA samples was calculated using the Eq. 2:

$$\chi_c (\%) = \frac{\Delta H_m - \Delta H_{cc}}{\Delta H_{\infty}} \times 100 \quad (2)$$

where ΔH_m and ΔH_∞ were the experimental melting enthalpies of each sample and the fully crystalline material, respectively, and ΔH_{cc} is the cold crystallization enthalpy, being the theoretical melting enthalpies for fully crystalline PLA (ΔH_∞) 93.1 J g⁻¹ (Beltrán et al., 2019) and fully crystalline PCL (ΔH_∞) 139.5 J g⁻¹ (Crescenzi et al., 1972). DSC and TGA analysis were performed in duplicate.

PLA, rPLA and rPLA-PCL control and active films were also analysed using modulated differential scanning calorimetry (MDSC) with Q2000 equipment (TA Instruments, USA) under nitrogen at a flow rate of 50 mL min⁻¹. 10 mg of sample was weighted in alumina pans and submitted to a heating from 10 to 220 °C with a heating rate of 2 °C min⁻¹, the modulation period 60 s, and the amplitude of modulation 0.32 °C. The glass transition temperature was recorded from the inflection point of the reversing heat flow signal.

2.5. Global and specific migration tests

Global migration tests of all developed films were conducted in order to verify the compliance with Regulation (EU) No 12/2011 related to plastic materials and articles intended to come into contact with food that affirms the overall migration (OM) limit must not exceed of the value of 10 mg of contaminants released per dm² of food contact surface (mg/dm²). For the test, two food simulants were used: food simulant A (Sim A: 10 % EtOH) that simulates hydrophilic food with pH above 4.5; and food simulant D1 (Sim D1: 50 % EtOH) for food with an alcohol content above 20 % and for oil-in-water emulsion (Regulation 10/2011). Rectangular strips of 0.15 dm² of each film were immersed in 25 mL of food simulant, respecting the specified surface-to-volume ratio of 6 dm² per kg of food for 10 days at 40 °C. At the end of the test period, each specimen was removed from the simulant. The simulant was then evaporated to dryness and the mass of the non-volatile residue was determined gravimetrically.

The release of quercetin from the active films was carried out by determining the specific migration from the films into the food simulants in accordance with the European Commission Regulation (EU) 2016/1416 (Regulation 2016/1416, 2016) the appropriate conditions and contact with food simulants were analyzed. As per the regulations, the relation of surface of film to volume of simulant was 6 dm² of film per 1 kg of simulant. The specific migration tests were performed using rectangular sections of 3 cm² of active samples (PLA3Q, rPLA3Q, 70rPLA30PCL3Q and 85rPLA15PCL3Q) immersed in 5 mL of two food simulants, Sim A and Sim D1, in triplicate for 10 days at 40 °C. Samples were collected after 1, 2, 4, 6, 24, 72 and 240 h. The release of quercetin was determined by using HPLC-DAD (1260 Infinity II Agilent). Chromatographic separations were achieved using a Zorbax Eclipse XDB-C18 (4.6 × 150 mm, 5 μm). The mobile phase consisted of solvent A (H₂O) and solvent B (MeOH) and pump supplied the following gradient program: 0–6 min, linear gradient from 10 % to 100 % solvent B and held for 4 min. The run time and flow were 10 min and 1 mL min⁻¹. The detection wavelength of quercetin was selected as 370 nm. The quercetin quantification was carried out based on calibration curves prepared in each simulant. The amount of quercetin released to the food simulant when using the different types of films as a function of time was calculated by the following equation:

$$q_t = \frac{(C_t - C_0) \cdot V}{m} \quad (3)$$

Where C_t is the concentration of quercetin at time t (mg L⁻¹), C₀ is the initial concentration of quercetin (mg L⁻¹), V is the volume of each food simulant (L) and m is the mass of film (kg).

The release process from the films was characterized using Fick's law considering the boundary conditions of the tests (López de Dicastillo et al., 2018). The release of the substances was controlled by the thermodynamic equilibrium condition, represented by the partition coefficient (K). K is defined as the ratio between the concentration of the analyte in the polymer phase and in the food simulant. This study assumed that the effective diffusion coefficient (D) for the mass transfer of quercetin remained constant and unaffected by both time and position. Because the simulant volume was finite and the antioxidant concentration was uniform, the proportion of antioxidant mass released in the food simulant over time can be mathematically represented as the following equation:

$$\frac{M(t)}{M(\infty)} = \left[1 - \frac{8}{\pi^2} \sum_{n=0}^{\infty} \frac{1}{(2n+1)^2} \exp\left(\frac{-D(2n+1)^2 \pi^2 t}{l^2}\right) \right] \quad (4)$$

where M(t) and M(∞) were the amount of the migrant in the food simulant at t time and at equilibrium, respectively, and l was the film thickness.

2.6. Antioxidant properties

ABTS (2,2'-azinobis(3-ethylbenzothiazoline-6-sulfonic acid) assay was employed to determine the antioxidant activity of films after their contact period with simulant. Control and active films were immersed into Sim A and D1 for 10 days, and subsequently, the antioxidant activity of food simulants was analyzed through the ABTS assay according to the method employed by Castro Lopez et al. (2013) with slight modifications (López de Dicastillo et al., 2015; Castro Lopez et al., 2013). ABTS^{•+} radical cationic solution was obtained by reacting 7 mM ABTS in water with 2.45 mM potassium persulfate and then stored in darkness at room temperature for 16 h. ABTS^{•+} radical solution was diluted to give an absorbance value of 1 at 734 nm (López de Dicastillo et al., 2015). On the other hand, 6 cm² pieces of each sample was immersed in 10 mL of food simulant in order to respect the area-volume ratio of 6 dm²/L for 10 days. Then 10 µL of simulant was mixed with 300 µL ABTS^{•+} radical solution and the reduction of the absorbance was analyzed. Antioxidant activities of the active materials were obtained as the percentage of inhibition values. The antioxidant activity (AA) results were expressed by using a calibration curve of gallic acid as the average value of mg of gallic acid equivalent (GAE)/ g of film ± standard deviation.

2.7. Data analysis

Statistical analysis was conducted using one-way analysis of variance (ANOVA). Significant differences among groups ($p < 0.05$) were assessed by Tukey's HSD post hoc test. All analyses were carried out using RStudio (version 2022.12.0 +353; RStudio, Boston, MA). Unless otherwise stated, the experiments were performed in triplicate, and the results are expressed as average value ± standard deviation.

3. Results and discussion

3.1. Optical properties of active films

Table 2 shows the color parameters of rPLA and their respective blends with PCL and Q. The color parameters of rPLA film ($a^* = -1.6$, $b^* = -0.89$) indicated a nearly neutral appearance with a slight greenish hue (see Fig. S1 in Supplementary material) associated with the inorganic green pigment present in the original water bottle. However, this coloration was not particularly evident due to the low thickness of the films, which minimized the visual perception of the tint. On the other hand, the addition of quercetin implied a significant increase of b^* values ($p < 0.05$) due to the intensified yellowish color of this flavonoid. Previous studies that incorporated Q as active compound have reported similar results due to its yellowish tone. Deng and Zhou (2024) in their study on a blend of PLA-Q and Lopez de Dicastillo et al. (2021) in their study on a complex active multilayer system containing Q, observed an

Table 2
Optical parameters of developed films.

Sample	L* (D65)	a* (D65)	b* (D65)	ΔE^*_{ab}
rPLA	18.92 ± 0.01 ^e	-1.60 ± 0.01	-0.89 ± 0.04 ^e	-
70rPLA30PCL	31.60 ± 0.05 ^d	-2.43 ± 0.01 ^b	-0.14 ± 0.05 ^e	12.71 ± 0.05 ^e
85rPLA15PCL	40.21 ± 0.10 ^b	-4.91 ± 0.04 ^c	1.60 ± 0.50 ^d	21.70 ± 0.04 ^d
rPLA3Q	40.10 ± 0.06 ^b	-12.80 ± 0.21 ^a	10.35 ± 0.10 ^c	26.47 ± 0.10 ^b
70rPLA30PCL 3Q	37.61 ± 0.15 ^c	-11.70 ± 0.13 ^d	12.62 ± 0.10 ^b	25.20 ± 0.13 ^c
85rPLA15PCL3Q	42.60 ± 0.03 ^a	-11.54 ± 0.10 ^d	15.00 ± 0.03 ^a	30.14 ± 0.01 ^a

^{a, b, ...}: different lowercase letters indicate differences for $p < 0.05$ between samples.

increase of b^* values and high ΔE difference (Deng, Zhou, 2024; Velásquez et al., 2019). Furthermore, considering a D65 illuminant and a 10 ° standard observer, the ΔE^*_{ab} values confirmed there were noticeable differences in color for the observer (see Figure S1 in Supplementary file).

3.2. Morphological analysis of developed films

Field emission scanning electron microscopy (FESEM) was used to observe the morphology of blended polymers by analyzing the cross-section of developed films. FESEM micrographs in Fig. 1 are presented at different magnifications to highlight morphological details. Particle size analysis was performed after scale calibration to ensure normalization and comparability among samples. As Fig. 1a and b show, rPLA films, both control and active, presented a homogenous matrix. Antioxidant rPLA3Q did not evidence Q agglomerates, confirming the good miscibility between the antioxidant and the post-consumer plastic. On the other hand, as Fig. 1c-f show, all blends exhibited spherical-shaped PCL particles surrounded by PLA matrix. Other studies have reported the same morphology of PCL when mixed within PLA matrix and a similar distribution, confirming the immiscibility between PLA and PCL polymers (Matta et al., 2014; Matumba et al., 2024). Fig. 1c-f display the cross-sectional morphology of the rPLA-PCL composites, and an inset graph has been added to illustrate the particle size distribution of the PCL spheres for both the control and the antioxidant-loaded samples of each blend.

Other works have reported the dispersion of PCL particles was found to be dependent on the blend ratio. At low PCL content (10–30 %), the distribution consisted of a simple dispersion of PCL particles into PLA matrix, which increased the toughness of the PLA (Matumba et al., 2024; Wachirahuttapong et al., 2016; Finotti et al., 2016; Jeon et al., 2018). Inserted graphs also indicate the average diameter of PCL particles, as a result of measuring an cross-sectional area of 610 µm². These values evidenced that, as PCL ratio increased and Q was added, the distribution and size of these particles turned more uniform and smaller. FESEM analysis was also used to investigate the distribution of the active compound, quercetin, within the blends. It was also evidenced that the surface of the polymer became more irregular when Q was added. Similar behavior was also observed by Ezati et al., on the fabrication of quercetin-loaded biopolymer films as functional packaging materials (Ezati & Rhim, 2021).

3.3. Thermal properties

The films were characterized by TGA and DSC to assess the effects of recycling and the incorporation of PCL and the natural flavonoid on the resulting thermal properties of developed ternary systems. Fig. 2a shows the thermal stability of the developed films analyzed by TGA. The main information obtained from the thermogram analysis is shown in Table 3. The onset temperature of degradation (T_{onset}) only presented significant differences between rPLA and the blend containing PCL at 15 %wt. Although some variations can be observed in the TGA curves shown in Fig. 2a, these correspond to individual measurements. When considering the averaged data, the differences in both the onset and the maximum degradation temperatures were slightly statistically and thermally significant, suggesting that the observed deviations are more likely related to material variability rather than to intrinsic differences in thermal stability among the samples.

In general, systems with PCL presented lower T_{onset} than pure PLA, and the addition of quercetin slightly delayed their thermal degradation, which could be related to its antioxidant effect. In the case of the first maximum degradation temperature (corresponding to PLA polymer), Q was observed to significantly increase the temperature of maximum degradation in the rPLA film, confirming the antioxidant and stabilizing effect of this flavonoid. These changes suggest that quercetin exhibited a stabilizing thermal effect, especially in recycled materials and blends,

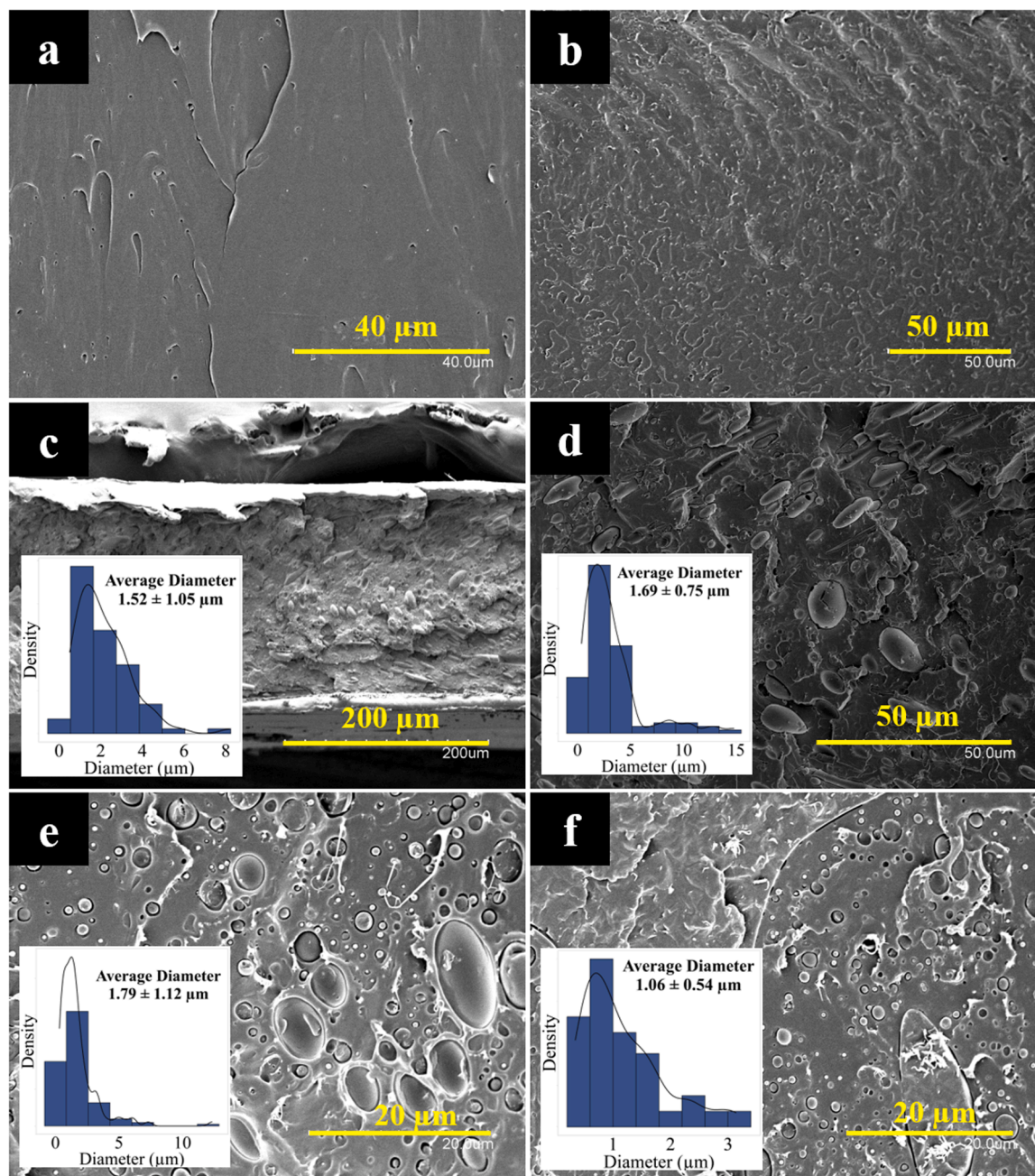


Fig. 1. SEM images of films. Surfaces images of rPLA a) and rPLA3Q b); Cross section images of 85rPLA15PCL c), 85rPLA15PCL3Q d), 70rPLA30PCL e) and 70rPLA30PCL3Q f), with density distribution of PCL spheres diameter on corresponding active blends.

due to its activity as a free radical inhibitor (Latos-Brozio et al., 2023). Quercetin is a flavonoid known for its high thermal stability. Q was also analyzed by TGA and the analysis confirmed that no degradation occurred at the melt-extrusion temperatures applied during blend processing (see [Supplementary material SM3](#)). This observation is consistent with previous studies in which quercetin was incorporated into polymeric matrices and no thermal degradation of the antioxidant was reported (López de Dicastillo et al., 2021; Lopez-de-Dicastillo et al., 2010). Finally, the final residue values were statistically different in films with or without the antioxidant. The residue levels in films without quercetin were below 1 %, while those containing quercetin were 1.70–2.40 %. This higher residue level may be associated with a higher quantity of non-aromatic compounds derived from quercetin that were thermoset at 700 °C.

The reduced thermal stability observed in rPLA compared to PLA is

likely due to the degradation of polymer chains during the simulated aging, mechanical recycling and further reprocessing, that led undoubtedly to a decrease in molecular weight (Arjona et al., 2026; Muñoz-Shugulí et al., 2025). These structural changes rendered the polymer more susceptible to thermal decomposition. Furthermore, the 85rPLA15PCL blend exhibited the lowest thermal stability among the composites, possibly due to the insufficient PCL content to provide a thermal stabilizing effect and the less favorable phase interaction between rPLA and PCL at this ratio (Mittal et al., 2015). Nevertheless, this effect was more pronounced at higher PCL ratio, as T_{onset} and $T_{max,1}$ of 70rPLA30PCL systems presented higher values, although the heterogeneity of materials was also the highest.

Control and active films were also studied through DSC analysis. [Fig. 2b](#) graphs the thermograms during the second heating process of developed films. During the second heating process, the samples

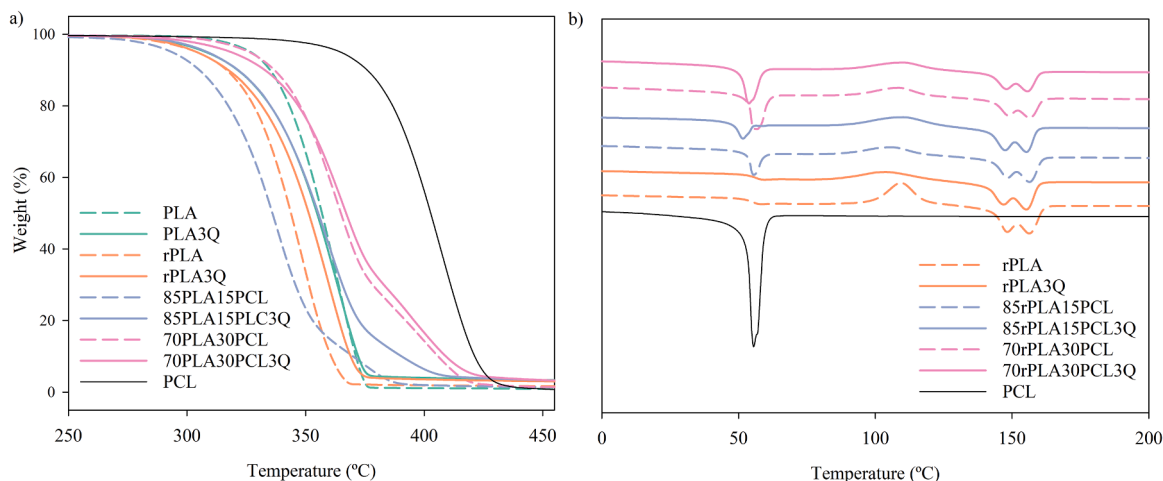


Fig. 2. a) Thermogravimetric analysis (TGA); and b) DSC thermograms of rPLA-based materials during second heating process.

Table 3

Thermal parameters from TGA of the PLA-based materials.

Sample	T _{onset} (°C)	T _{max, 1} (°C)	T _{max, 2} (°C)	Residue at 800 °C (%)
PLA	342.9 ± 4.1 ^a	366.0 ± 3.2 ^a	-	0.30 ± 0.03 ^a
PLA3Q	333.8 ± 1.4 ^{ab}	363.6 ± 1.7 ^a	-	2.16 ± 0.15 ^b
rPLA	324.2 ± 1.5 ^{ab}	348.8 ± 0.4 ^{ab}	-	0.40 ± 0.06 ^a
rPLA3Q	335.7 ± 6.5 ^{ab}	362.4 ± 3.7 ^{ab}	-	1.70 ± 0.33 ^b
85rPLA15PCL	312.3 ± 1.6 ^b	336.7 ± 1.8 ^b	373.0 ± 4.7 ^a	0.55 ± 0.04 ^a
85rPLA15PCL3Q	321.8 ± 12.3 ^{ab}	351.6 ± 9.7 ^{ab}	388.2 ± 8.4 ^{ab}	2.39 ± 0.31 ^b
70rPLA30PCL	330.0 ± 14.4 ^{ab}	353.8 ± 13.1 ^{ab}	399.4 ± 8.5 ^b	0.64 ± 0.13 ^a
70rPLA30PCL3Q	332.7 ± 9.7 ^{ab}	360.1 ± 7.3 ^{ab}	394.3 ± 0.6 ^{ab}	2.01 ± 0.44 ^b
PCL	382.8 ± 0.8 ^c	-	407.5 ± 0.1 ^b	0.10 ± 0.13 ^a

^{a, b, ...}: different lowercase letters indicate differences for $p < 0.05$ between samples in the same thermal properties.

exhibited similar thermal events: a glass transition temperature at approx. 55 °C, an exotherm process corresponding to the cold crystallization of PLA at approximately 110 °C, and a melting endotherm process that peaked at 155 °C (Zhang et al., 2018). DSC results revealed significant differences in the thermal and crystalline PLA behavior of the materials. The recycling process of rPLA did not cause significant changes in T_g or T_m, suggesting that the basic thermal properties of this polymer remained stable after recycling and reprocessing. However, an increase in PLA crystallinity was observed in rPLA compared to original PLA-based bottle. This trend could be attributed to a reduction in PLA molar mass, which favored chain mobility and, therefore, their reorganization into crystalline structures during cooling. In addition, the incorporation of Q exhibited various effects into the polymer matrix. When added to PLA from commercial water bottles (PLA3Q), a slight increase in T_g was observed, which could indicate an interaction of the antioxidant with the polymer chains, restricting their mobility. In the case of the post-consumer recycled rPLA and blends with PCL, the addition of Q caused a more marked reduction in T_g, possibly due to a plasticizing effect or greater compatibility between the phases (Moraczewski et al., 2025). Furthermore, the presence of Q in systems such as rPLA3Q resulted in greater PLA crystallinity, indicating a possible nucleating effect of the antioxidant. The percentage of PCL was

crucial for the crystallinity of the films due to differences in compatibility with the matrix (Ferri et al., 2016). Therefore, it was necessary to analyze the thermal properties of PCL in the films composed by the blends. Because the glass transition of PLA and melting process of PCL occurred relatively at similar range of temperatures, the relative PCL crystallinity values was analyzed by modulated DSC (MDSC), whose thermograms curves are presented in Fig. 3 and results are shown in Table 4. MDSC analysis exhibited the total heat flow and the total heat flow separated into two signals. The reversing curves in blue represented the component of the total heat that depend on the heating rate, that is, it is in phase with the modulated heating. Meanwhile, the non-reversing curves in red depended only on the absolute temperature and are out of phase with modulated heating (López-de-Dicastillo et al., 2025). As observed in Table 4, the crystallinity of PCL remained relatively high in all blends, although a slight decrease was observed when quercetin was incorporated into the mixture containing 15 %wt. PCL, which could indicate some interference between both species in the crystallization process. In summary, the combination of recycling and the addition of quercetin shows a notable tendency toward the increase of PLA crystallinity, which could be due to a synergy between thermal processing and the effect of the additive.

In the blends, the balance between the amorphous phase of rPLA and the semi-crystallinity of PCL appeared to depend on both the PCL ratio and the presence of quercetin, which in some cases could act as a compatibilizer or structural modifier, affecting the thermal transitions of both components.

Overall, the results indicated that the thermal properties of rPLA can be significantly modulated through recycling, blending with PCL, and the incorporation of antioxidants. The combination of these strategies is particularly relevant for optimizing the crystallinity and thermal transitions of the material, depending on the desired application.

3.4. Global and specific migration results

The overall migration (OM) values of developed films are presented in Fig. 4. All samples complied with the regulatory OM limit of 10 mg dm⁻² across both food simulants, except for film 70rPLA30PCL3Q exposed to simulant D1, due to the specific migration of Q. In fact, all samples with antioxidant compounds in the formulation exhibited higher OM values compared to their control samples. It must be considered that the total migration also included the quantity of the active substance. A similar trend was reported by Plackett et al. (2006) in their study on the characterization of a blend of L-Poly-lactide-Polycaprolactone. They evaluated the overall migration in several food simulants. The OM values for the simulant A (10 % v/v ethanol) were low and consistent with our results, stating that the

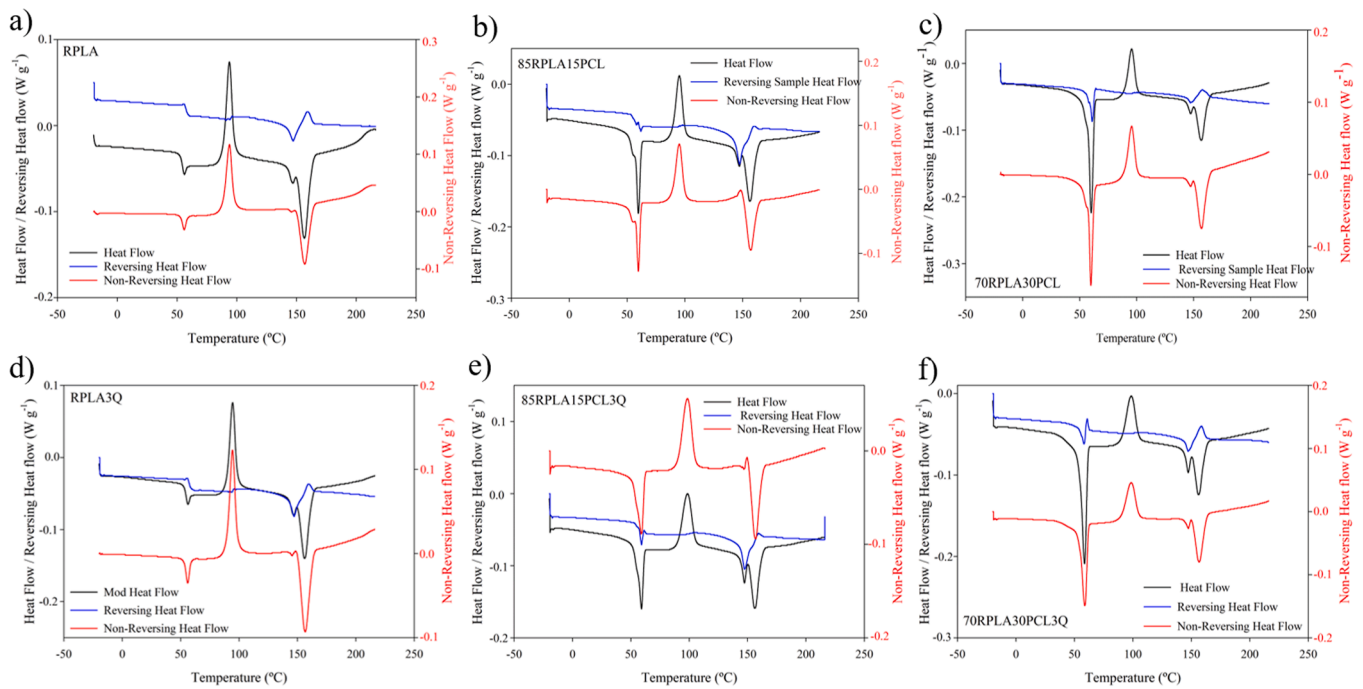


Fig. 3. Representative MDSC curves of reversing heat flow (HF), non-reversing HF, and modulated HF of some rPLA-based films: a) rPLA, b) 85rPLA15PCL, c) 70rPLA30PCL, d) rPLA3Q, e) 85rPLA15PCL3Q and f) 70rPLA30PCL3Q.

Table 4

Thermal parameters from DSC thermograms of the PLA-based materials during the second heating process.

Film	PLA						PCL		
	T_g (°C)	T_{CC} (°C)	ΔH_{CC} (J/g)	T_m (°C)	ΔH_m (J/g)	$\chi_{c,PLA}$ (%)	ΔH_m (J/g)	$\chi_{c,PCL}$ (%)	
PLA	55.58 ± 0.61^{ab}	107.9 ± 0.1^{ab}	29.48 ± 0.14	156.3 ± 0.1^{ab}	34.4 ± 0.6	5.3 ± 0.5^d	-	-	
PLA3Q	56.44 ± 0.57^a	106.6 ± 0.7^b	17.14 ± 0.59	155.6 ± 0.2^c	30.9 ± 0.3	15.2 ± 1.0^b	-	-	
rPLA	55.14 ± 0.16^{ab}	109.4 ± 0.1^{ab}	26.01 ± 1.02	156.2 ± 0.1^{ab}	35.3 ± 0.3	9.9 ± 0.8^c	-	-	
rPLA3Q	56.07 ± 0.94^{ab}	102.6 ± 1.4^c	12.62 ± 1.50	155.2 ± 0.1^c	33.9 ± 0.2	23.6 ± 1.8^a	-	-	
85rPLA15PCL	54.55 ± 0.16^b	106.3 ± 0.8^b	11.80 ± 0.20	156.3 ± 0.2^a	28.6 ± 0.6	24.9 ± 1.1^a	9.5 ± 0.2	43.5 ± 4.9	
85rPLA15PCL3Q	50.22 ± 0.04^c	110.6 ± 0.7^a	16.25 ± 0.02	155.3 ± 0.1^c	28.1 ± 0.4	18.3 ± 0.7^b	5.9 ± 0.3	28.2 ± 1.2	
70rPLA30PCL	54.65 ± 0.14^b	108.1 ± 0.8^{ab}	11.76 ± 0.12	156.3 ± 0.2^a	23.0 ± 0.3	24.6 ± 0.6^b	18.3 ± 1.9	43.7 ± 4.6	
70rPLA30PCL3Q	52.31 ± 0.25^d	110.6 ± 0.6^a	12.49 ± 0.49	155.7 ± 0.1^{ab}	22.6 ± 1.1	23.3 ± 1.3^b	18.2 ± 2.0	43.5 ± 4.9	
PCL	-	-	-	-	-	-	70.3 ± 2.8	50.4 ± 2.0	

^{a, b, ...}: different lowercase letters indicate differences for $p < 0.05$ between samples in the same thermal properties.

migration in neutral aqueous liquids is very low (Plackett et al., 2006). Quercetin release studies were carried out by exposure of the films developed to food simulants included in EU regulations (López de Dicastro et al., 2011).

The higher overall migration observed in the 70rPLA30PCL3Q film compared to the 85rPLA15PCL3Q film can be explained by the increased PCL content in the blend. A higher PCL ratio leads to a more amorphous structure and greater free volume, which enhances the mobility of quercetin molecules and facilitates their release. In contrast, the lower PCL content in the 85rPLA15PCL3Q film results in a more compact matrix with reduced molecular mobility, limiting the migration of the active compound. This trend is also reflected in the specific migration profiles shown in Figs. 5a and 5b.

As Fig. 5a and b show, the Q release profile of active developed films exhibited an exponential growth until reaching a maximum, where release equilibrium was established. In Sim A, this growth indicated that both original and recycled PLA films exhibited lower Q release than those composed by blends. Moreover, their migration were slower, as equilibrium was not reached during the initial hours, as it occurred for PLAPCLQ blends. The type of food simulant was also a factor of difference in the Q release. When comparing the migration data across both simulants, higher maximum Q releases were observed in the presence of

a greater proportion of ethanol, specifically, when the films were immersed in Sim D1 (50 % ethanol). This behavior depends on the affinity between the migrant and the simulant, which can be described by K . These values are shown in Fig. 5c and d. K and diffusion coefficients (D) were strongly influenced by both the type of food simulant and the polymer formulation. Quercetin is highly soluble in ethanol (2 mg mL^{-1}), and therefore, K values were much lower when migrating in Sim D1. This behavior underlines the higher affinity of Q for a medium with a high proportion of ethanol, thus facilitating its release. PLA3Q and rPLA3Q exhibited the highest K values in both simulants, indicating that quercetin remained mostly retained in the polymer matrix, resulting in lower release. In contrast, active blended films (70rPLA30PCL3Q and 85rPLA15PCL3Q) showed significantly lower K values, suggesting reduced retention of Q due to a lower affinity between the polymer matrix and the antioxidant. This greater release correlates with an increase in the mobility of the polymer chains with respect to the control polymers (PLA3Q and rPLA3Q) as it was previously reported in Section 3.4 as a decrease in T_g . In Sim D1, all formulations presented significantly lower K values, particularly in PLA-based films, where their value decreased up to 10-fold. This behavior reflects the greater affinity of K for the medium richer in ethanol. In the case of blends, the reduction was even more drastic, with the release

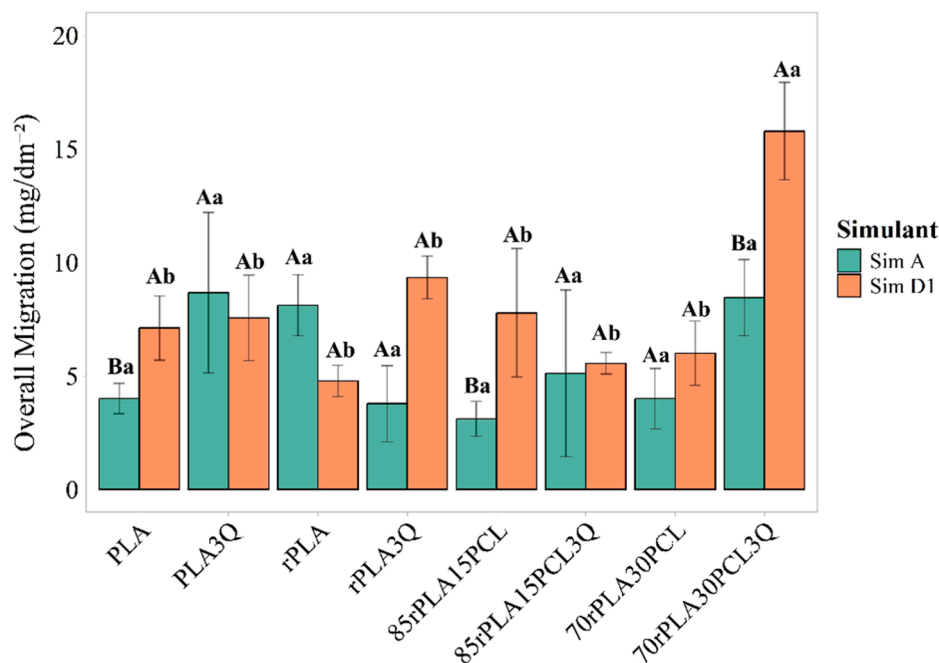


Fig. 4. Overall migration test of samples in Sim A and D1. Lowercase letters a and b indicate differences for $p < 0.05$ between samples in the same simulant; Capital letters A and B indicate differences for $p < 0.05$ between simulants of the same sample.

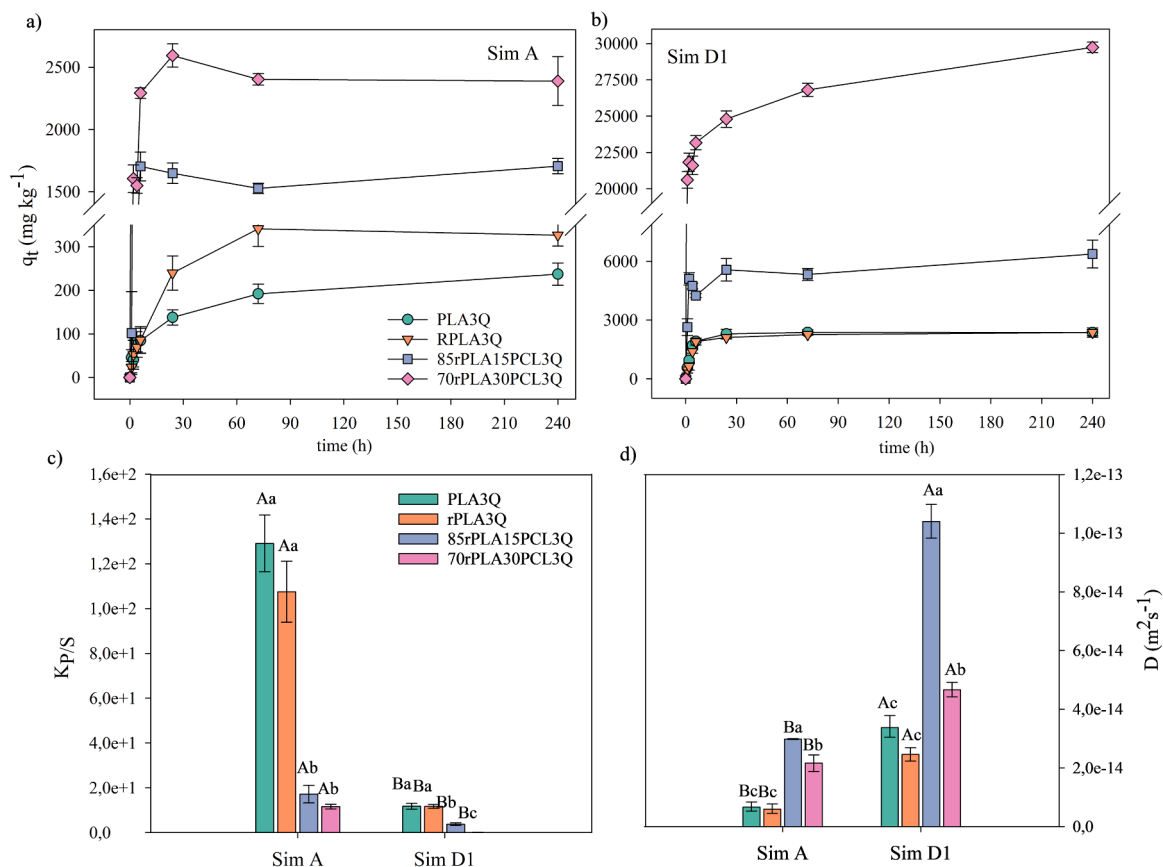


Fig. 5. Quercetin release kinetics into: a) Sim A; and b) Sim D1; and c) Partition (K); and d) Diffusion (D) coefficient values for the release of Q from developed active films into the food simulants tested. ^{a, b,...}: different lowercase letters indicate differences for $p < 0.05$ between samples in the same simulants; ^{A, B,...}: different capital letters indicate differences for $p < 0.05$ between simulants in the same samples.

approaching complete extraction, since the K values were very close to 0. There were significant differences between copolymers with different

PCL compositions in Sim D1, unlike what was observed in Sim A. This distinction lies in the intensification of the PCL effect in the presence of a more extractive medium, amplifying the impact of the PCL content. The highest PCL ratio contributed with an increase in the free volume available in the polymer matrix, creating more space for the movement of quercetin chains and molecules (Ferreira Marques et al., 2008).

Fig. 5d also exhibits that the type of simulant also influenced the quercetin release kinetics, processes described by the diffusion coefficient (D) and defined by Fick's laws. This parameter is essential for characterizing the rate of molecular transport through the polymer. In this case, this antioxidant diffused from the film matrix through the interface to the surrounding medium. When the material is considered a flat film of constant thickness, the release kinetics can be characterized by an apparent diffusion coefficient according to the solution of Fick's second law (Vidal et al., 2022; Rojas et al., 2021). As can be seen in Fig. 5, in Sim A, all films presented very low values, indicating very limited molecular mobility and restricted Q diffusion. However, when using Sim D1, a significant increase in diffusion was observed in all formulations. The blend composed by 70/30 rPLA/PCL ratio showed the highest D coefficient, followed by 85/15 rPLA/PCL blend, and finally by the PLA and rPLA films. This increase suggested that ethanol promoted the swelling of the polymer matrix (Kirchkeszner et al., 2022) and reduced the barrier properties, thus facilitating the mobility of quercetin molecules. Furthermore, the higher diffusion in the blends with PCL could be attributed to the more amorphous structure and the greater free volume, which promoted molecular transport within the film.

3.5. Antioxidant activity of developed active materials

Fig. 6 presents the antioxidant activity (AA) expressed as mg GAE per g film after 10 days of contact in both food simulants. The results were in agreement with those of the specific migration of Q in the food simulants. A correlation between AA and the release of active compound has also been reported in other studies investigating the AA of active films after contact with food simulants (Castro López et al., 2013; Velásquez et al., 2019). The effect of simulant composition was significantly noticeable ($p < 0.05$). The highest amount of Q was released in Sim D1, which turn, coincided with the highest antioxidant activity values

achieved when compared to Sim A. This can be attributed to the affinity of this antioxidant compound by ethanol. Furthermore, as in the case of specific migration for PLA3Q and rPLA3Q, the lower release of Q resulted in lower antioxidant activities compared to the blend samples.

The ABTS assay evaluates the antioxidant capacity by monitoring the reduction of the blue-green ABTS^{•+} radical cation to its colorless form. The antioxidant mechanism of Q in the ABTS assay involves both single electron transfer (SET) and hydrogen atom transfer (HAT) pathways (Prior & Schaich, 2005; Platzer et al., 2022). The high antioxidant activity of this flavonoid is mainly attributed to its multiple hydroxyl groups, particularly the catechol structure in the B-ring, which facilitates both electron and hydrogen atom donation (Zeng et al., 2020). Quercetin is classified as a moderately fast-reacting antioxidant in the ABTS assay, with rapid initial scavenging phase followed by a slower reaction stage, reflecting an efficient but non-instantaneous interaction with ABTS^{•+} radicals (Ilyasov et al., 2018). By donating electrons or hydrogen atoms to neutralize reactive oxygen and nitrogen species (ROS/RNS), such as superoxide, hydroxyl, and peroxy radicals, quercetin effectively interrupts lipid peroxidation chain reactions, which are primarily responsible for rancidity, off-flavors, and color changes in lipid-rich foods, such as meat, fish, and edible oils. Through radical stabilization, quercetin contributes to the preservation of food quality and the extension of shelf life (Gutiérrez-del-Río et al., 2021)

In the present formulations, the chemical nature of this recycled polymer, characterized by a highly branched molecular structure designed to provide suitable rheological properties for extrusion, injection, and blow moulding processes, confers promising potential for applications in predominantly rigid food packaging produced via melt-mixing techniques. In particular, two main active packaging formats can be envisaged: trays manufactured by extrusion followed by thermoforming, and containers such as tubs, cups, or bottles obtained by injection or blow moulding.

4. Conclusions

Mechanical recycling of post-consumer PLA represents a valid alternative for end-of-life management of this bioplastic, contributing to the valorization of post-consumer PLA (rPLA) packaging. This work

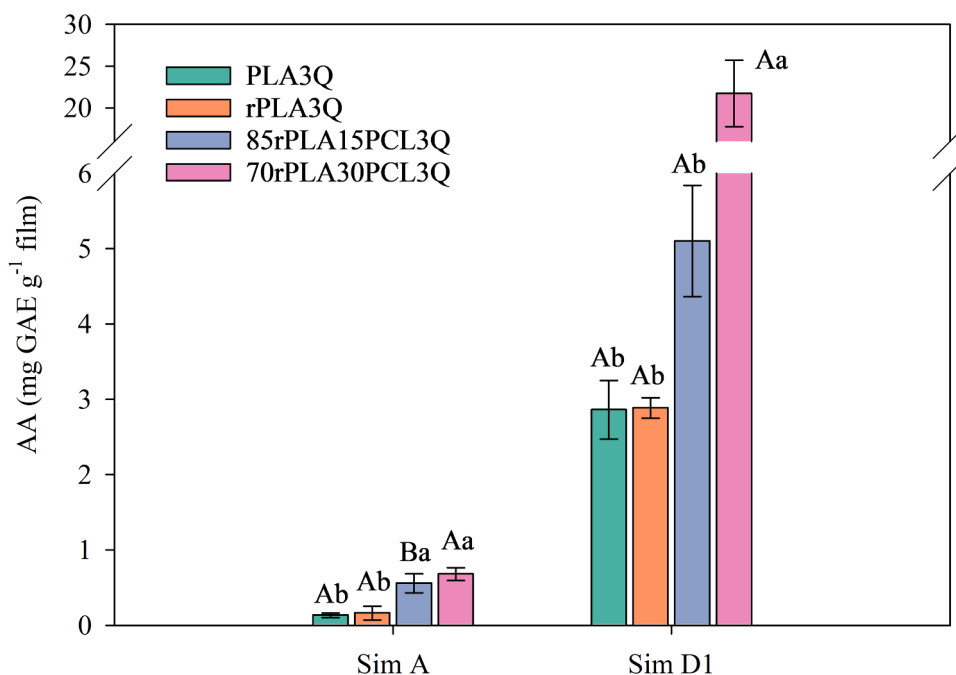


Fig. 6. Antioxidant activity of active sample in both food simulants D1 and A. ^{a, b, ...}: different lowercase letters indicate differences for $p < 0.05$ between samples in the same simulants. ^{A, B, ...}: different capital letters indicate differences for $p < 0.05$ between simulants in the same samples.

demonstrated that post-consumer PLA from commercial water bottles can be successfully mechanically recycled and reprocessed into functional active packaging materials. Blending rPLA with PCL and incorporating 3 wt% quercetin significantly modified the structural and functional behavior of the films. Recycling did not alter the main thermal transitions of PLA, although rPLA exhibited a higher crystallinity (from 5.3 % in PLA to 9.9 % in rPLA). The addition of PCL further increased PLA crystallinity up to ~25 % in the 70rPLA30PCL blend. Quercetin also contributed to crystallinity enhancement, reaching 23.6 % in rPLA3Q. The release of quercetin depended strongly on blend composition and simulant polarity. In food simulant D1, the maximum released amount increased from approx. 3 mg Q/g film (PLA3Q and rPLA3Q) to 6 mg Q/g film (85rPLA15PCL3Q) and 30 mg Q/g film (70rPLA30PCL3Q). This enhanced release resulted in correspondingly higher antioxidant activity, reaching up to 24 mg GAE/g 70rPLA30PCL3Q film, nearly eight times higher than that of PLA3Q and rPLA3Q. Among all formulations, 70rPLA30PCL3Q exhibited the best overall performance, combining the highest quercetin release and strongest antioxidant effect, particularly in fatty-food simulant D1. These findings confirmed that mechanically recycled PLA can be upcycled into efficient active packaging materials by tailoring PCL content and antioxidant incorporation. Future research could incorporate controlled mechanical loading to better emulate practical service scenarios and should evaluate potential migrants originating from the recycled polymer, assess mechanical and barrier performance under real food storage conditions, and further optimize release profiles depending on the target food product.

Funding

This work was funded by Hijos de Rivera Co.

CRedit authorship contribution statement

José Manuel López Vilarino: Writing – original draft, Resources. **Sara Exojo-Trujillo:** Writing – original draft, Validation, Methodology, Formal analysis, Data curation. **Andrea Feroce:** Writing – review & editing, Writing – original draft, Validation, Methodology, Formal analysis, Data curation. **Lopez de Dicastillo Carol:** Writing – review & editing, Writing – original draft, Supervision, Project administration, Methodology, Investigation, Funding acquisition, Conceptualization. **Rafael Gavara:** Writing – original draft, Supervision. **Fabio Licciardello:** Writing – original draft, Funding acquisition.

Declaration of Competing Interest

The authors declare that they have no conflict of interests.

Acknowledgments

The authors acknowledge the award of the Spanish government MCIU/AEI to the IATA-CSIC as Center of Excellence Accreditation Severo Ochoa (CEX2021-001189-S/MCIU/AEI/10.13039/501100011033).

Appendix A. Supporting information

Supplementary data associated with this article can be found in the online version at [doi:10.1016/j.fpsl.2026.101700](https://doi.org/10.1016/j.fpsl.2026.101700).

Data availability

Data will be made available on request.

References

- Agüero, Á., Corral Perianes, E., Abarca de las Muelas, S. S., Lascano, D., de la Fuente García-Soto, M. D. M., Peltzer, M. A., Balart, R., & Arrieta, M. P. (2023). Plasticized mechanical recycled PLA films reinforced with microbial cellulose particles obtained from Kombucha fermented in Yerba Mate Waste. *Polymers*, 15(2), 285. <https://doi.org/10.3390/polym15020285>
- Arjona, P., Velásquez, E., López-Carballo, G., Hernández-Muñoz, P., Gavara, R., & López-de-Dicastillo, C. (2026). Simulated secondary mechanical recycling of PLA water bottles: Insights into structural integrity, barrier performance, and biodegradability. *Resources, Conservation and Recycling*, 225, Article 108597. <https://doi.org/10.1016/j.resconrec.2025.108597>
- Arrieta, M. P. (2021). Influence of plasticizers on the compostability of polylactic acid. *Journal of Applied Research in Technology Engineering*, 2(1), 1–9. <https://doi.org/10.4995/jarte.2021.14772>
- Badia, J. D., Gil-Castell, O., & Ribes-Greus, A. (2017). Long-term properties and end-of-life of polymers from renewable resources. *Polymer Degradation and Stability*, 137, 35–57. <https://doi.org/10.1016/j.polydegradstab.2017.01.002>
- Beltrán, F. R., Barrio, I., Lorenzo, V., Del Río, B., Martínez Urreaga, J., & de La Orden, M. U. (2019). Valorization of poly (lactic acid) wastes via mechanical recycling: Improvement of the properties of the recycled polymer. *Waste Management Research*, 37(2), 135–141. <https://doi.org/10.1177/0734242X18798448>
- Castro-Aguirre, E., Iniguez-Franco, F., Samsudin, H., Fang, X., & Auras, R. (2016). Poly (lactic acid)—Mass production, processing, industrial applications, and end of life. *Advanced Drug delivery Reviews*, 107, 333–366. <https://doi.org/10.1016/j.addr.2016.03.010>
- Castro Lopez, M. D. M., Lopez de Dicastillo, C., Lopez Vilarino, J. M., & Gonzalez Rodriguez, M. V. (2013). Improving the capacity of polypropylene to be used in antioxidant active films: Incorporation of plasticizer and natural antioxidants. *Journal of Agricultural and Food Chemistry*, 61(35), 8462–8470. <https://doi.org/10.1021/jf402670a>
- Cosate de Andrade, M. F., Souza, P. M., Cavalett, O., & Morales, A. R. (2016). Life cycle assessment of poly (lactic acid)(PLA): Comparison between chemical recycling, mechanical recycling and composting. *Journal of Polymers and the Environment*, 24, 372–384. <https://doi.org/10.1007/s10924-016-0787-2>
- Crescenzi, V., Manzini, G., Calzolari, G., & Borri, C. (1972). Thermodynamics of fusion of poly(fl-propiolactone) and poly(ε-caprolactone). Comparative analysis of the melting of aliphatic polylactone and polyester chains. *European Polymer Journal*, 8, 449–463.
- Deng, P., & Zhou, Y. (2024). A sustainable strategy for promoting the colour strength and ultraviolet/oxidation resistance of polylactic acid fabric integrating quercetin and food-grade ester. *Industrial Crops and Products*, 208, Article 117875. <https://doi.org/10.1016/j.indcrop.2023.117875>
- EC- European Commission. (2019). *Communication from the Commission, The European Green Deal*. COM(2019) 640 final. Brussels, Belgium: European Commission (<https://eur-lex.europa.eu/legal-content/EN/TXT/?uri=CELEX:52019DC0640>). COM (2019) 640 final.
- EC- European Commission. (2020). *A new Circular Economy Action Plan*. Brussels, Belgium: European Commission. (<https://eur-lex.europa.eu/legal-content/EN/TXT/?uri=CELEX%3A52020DC0098>) (accessed on 22 January 2025).
- EC- European Commission. (2022). *EU policy framework on biobased, biodegradable and compostable plastics*. Brussels, Belgium: European Commission. (https://environment.ec.europa.eu/publications/communication-eu-policy-framework-biobased-biodegradable-and-compostable-plastics_en) (accessed on 22 January 2025).
- Ezati, P., & Rhim, J. W. (2021). Fabrication of quercetin-loaded biopolymer films as functional packaging materials. *ACS Applied Polymer Materials*, 3(4), 2131–2137. <https://doi.org/10.1021/acsapm.1c00177>
- Ferreira Marques, M., Gordo, P., de Lima, A., Queiroz, D., Norberta de Pinho, M., Major, P., & Kajcsos, Z. (2008). Free-volume studies in polycaprolactone/poly (propylene oxide) urethane/urea membranes by positron lifetime spectroscopy. *Acta Physica Polonica A*, 113(5), 1359–1364. <https://doi.org/10.12693/APhysPolA.113.1359>
- Ferri, J. M., Fenollar, O., Jorda-Vilaplana, A., García-Sanoguera, D., & Balart, R. (2016). Effect of miscibility on mechanical and thermal properties of poly(lactic acid)/ polycaprolactone blends. *Polymer International*, 65, 453–463. <https://doi.org/10.1002/pi.5079>
- Finotti, P. F., Costa, L. C., & Chinelatto, M. A. (2016). Effect of the chemical structure of compatibilizers on the thermal, mechanical and morphological properties of immiscible PLA/PCL blends. In *Macromolecular Symposia*, 368(1), 24–29. <https://doi.org/10.1002/masy.201600056>
- Geyer, R., Jambeck, J. R., & Law, K. L. (2017). Production, use, and fate of all plastics ever made. *Science Advances*, 3(7), Article e1700782. <https://doi.org/10.1126/sciadv.1700782>
- Gutiérrez-del-Río, I., López-Ibáñez, S., Magadán-Corpas, P., Fernández-Calleja, L., Pérez-Valero, A., Tuñón-Granda, M., Migúlez, E. M., Villar, C. J., & Lombó, F. (2021). Terpenoids and polyphenols as natural antioxidant agents in food preservation. *Antioxidants*, 10(8), 1264. <https://doi.org/10.3390/antiox10081264>
- Hahladakis, J. N., Velis, C. A., Weber, R., Iacovidou, E., & Purnell, P. (2018). An overview of chemical additives present in plastics: Migration, release, fate and environmental impact during their use, disposal and recycling. *Journal of Hazardous Materials*, 344, 179–199. <https://doi.org/10.1016/j.jhazmat.2017.10.014>
- Haq, R. H. A., Rahman, M. N. A., Ariffin, A. M. T., Hassan, M. F., Yunus, M. Z., & Adzila, S. (2017). Characterization and Mechanical Analysis of PCL/PLA composites for FDM feedstock filament. In *IOP Conference Series: Materials Science and Engineering*, 226(1), Article 012038. <https://doi.org/10.1088/1757-899X/226/1/012038>

- Ilyasov, I. R., Beloborodov, V. L., & Selivanova, I. A. (2018). Three ABTS•+ radical cation-based approaches for the evaluation of antioxidant activity: fast- and slow-reacting antioxidant behavior. *Chemical Papers*, 72, 1917–1925. (<https://link.springer.com/article/10.1007/s11696-018-0415-9>).
- Jain, S., Reddy, M. M., Mohanty, A. K., Misra, M., & Ghosh, A. K. (2010). A new biodegradable flexible composite sheet from poly (lactic acid)/poly (ϵ -caprolactone) blends and Micro-Talc. *Macromolecular Materials and Engineering*, 295(8), 750–762. <https://doi.org/10.1002/mame.201000063>
- Jannathia, N., & Gutiérrez, T. J. (2025). Recycling and revalorization of PLA and PHA-based food packaging waste: A review. *Sustainable Materials and Technologies*, 44, Article e01364. <https://doi.org/10.1016/j.susmat.2025.e01364>
- Jasrotia, S., Gupta, S., Kudipady, M. L., & Puttaiahgowda, Y. M. (2025). Advancing food preservation with quercetin-based Nanocomposites: Antimicrobial, antioxidant, and controlled-release strategies - A review. *Current Research in Food Science*, 11, Article 101159. <https://doi.org/10.1016/j.crf.2025.101159>
- Jeon, J. S., Han, D. H., & Shin, B. Y. (2018). Improvements in the rheological properties, impact strength, and the biodegradability of PLA/PCL blend compatibilized by electron-beam irradiation in the presence of a reactive agent. *Advances in Materials Science and Engineering*, 2018(1), Article 5316175. <https://doi.org/10.1155/2018/5316175>
- Kemala, T., Budianto, E., & Soegiyono, B. (2012). Preparation and characterization of microspheres based on blend of poly (lactic acid) and poly (ϵ -caprolactone) with poly (vinyl alcohol) as emulsifier. *Arabian Journal of Chemistry*, 5(1), 103–108. <https://doi.org/10.1016/j.arabjc.2010.08.003>
- Kirchkeszner, C., Petrovics, N., Tábi, T., Magyar, N., Kovács, J., Szabó, B. S., Nyiri, Z., & Eke, Z. (2022). Swelling as a promoter of migration of plastic additives in the interaction of fatty food simulants with poly(lactic acid) and polypropylene-based plastics. *Food Control*, 132, Article 108354. <https://doi.org/10.1016/j.foodcont.2021.108354>
- Latos-Brozio, M., Masek, A., & Piotrowska, M. (2023). Effect of enzymatic polymerization on the thermal stability of flavonoids. *Journal of Thermal Analysis and Calorimetry*, 148, 5357–5374. <https://doi.org/10.1007/s10973-023-12089-1>
- López-de-Dicastillo, C., Velásquez, E., Rojas, A., Higuera, L., Hernández-Muñoz, P., & Gavara, R. (2025). Designing novel waterborne poly(lactic acid) coatings for food packaging applications including poly(vinyl alcohol) as stabilizer. *Food Packaging and Shelf Life*, 49, Article 101493. <https://doi.org/10.1016/j.fpsl.2025.101493>
- López de Dicastillo, C., Garrido, L., Velásquez, E., Rojas, A., & Gavara, R. (2021). Designing biodegradable and active multilayer system by assembling an electrospun polycaprolactone mat containing quercetin and nanocellulose between poly(lactic acid) films. *Polymers*, 13(8), 1288. <https://doi.org/10.3390/polym13081288>
- López de Dicastillo, C., Villegas, C., Garrido, L., Roa, K., Torres, A., Galotto, M. J., Rojas, A., & Romero, J. (2018). Modifying an active compound's release kinetic using a supercritical impregnation process to incorporate an active agent into PLA electrospun mats. *Polymers*, 10(5), 479. <https://doi.org/10.3390/polym10050479>
- López de Dicastillo, C., Navarro, R., Guada, A., & Galotto, M. J. (2015). Development of biocomposites with antioxidant activity based on red onion extract and acetate cellulose. *Antioxidants*, 4(3), 533–547. <https://doi.org/10.3390/antiox4030533>
- López de Dicastillo, C., Nerín, C., Alfaro, P., Catalá, R., Gavara, R., & Hernández-Muñoz, P. (2011). Development of new antioxidant active packaging films based on ethylene vinyl alcohol copolymer (EVOH) and green tea extract. *Journal of Agricultural and Food Chemistry*, 59(14), 7832–7840. <https://doi.org/10.1021/jf201246g>
- Lopez-de-Dicastillo, C., Alonso, J. M., Catala, R., Gavara, R., & Hernandez-Munoz, P. (2010). Improving the antioxidant protection of packaged food by incorporating natural flavonoids into ethylene–vinyl alcohol copolymer (EVOH) films. *Journal of Agricultural and Food Chemistry*, 58(20), 10958–10964. <https://doi.org/10.1021/jf1022324>
- Matta, A. K., Rao, R. U., Suman, K. N. S., & Rambabu, V. (2014). Preparation and characterization of biodegradable PLA/PCL polymeric blends. *Procedia Materials Science*, 6, 1266–1270. <https://doi.org/10.1016/j.mspro.2014.07.201>
- Matumba, K. I., Mokheba, T. C., Ojijo, V., Sadiku, E. R., & Ray, S. S. (2024). Morphological characteristics, properties, and applications of polylactide/poly (ϵ -caprolactone) blends and their composites—a review. *Macromolecular Materials and Engineering*, Article 2400056. <https://doi.org/10.1002/mame.202400056>
- Maurizzi, E., Bigi, F., Quartieri, A., De Leo, R., Volpelli, L. A., & Pulvirenti, A. (2022). The green era of food packaging: General considerations and new trends. *Polymers*, 14(20), 4257. <https://doi.org/10.3390/polym14204257>
- Mittal, V., Akhtar, T., & Matsko, N. (2015). Mechanical, thermal, rheological and morphological properties of binary and ternary blends of PLA, TPS and PCL. *Macromolecular Materials and Engineering*, 300, 423–435. <https://doi.org/10.1002/mame.201400332>
- Moraczewski, K., Stepczyńska, M., Raszewska-Kaczor, A., Szymańska, L., & Rytlewski, P. (2025). PLA/PCL polymer material for food packaging with enhanced antibacterial properties. *Polymers*, 17, 1134. <https://doi.org/10.3390/polym17091134>
- Muñoz-Shugulí, C., Morán, D., Velásquez, E., López-Vilariño, J. M., & López-de-Dicastillo, C. (2025). Effect of degradation during multiple primary mechanical recycling processes on the physical properties and biodegradation of commercial PLA-based water bottles. *Polymers*, 17, 2542. <https://doi.org/10.3390/polym17182542>
- Ncube, L. K., Ude, A. U., Ogunmuyiwa, E. N., Zulkifli, R., & Beas, I. N. (2021). An overview of plastic waste generation and management in food packaging industries. *Recycling*, 6(1), 12. <https://doi.org/10.3390/recycling6010012>
- Plackett, D. V., Holm, V. K., Johansen, P., Ndoni, S., Nielsen, P. V., Sipilainen-Malm, T., Södergård, A., & Verstichel, S. (2006). Characterization of l-poly(lactide) and l-poly(lactide–polycaprolactone) co-polymer films for use in cheese-packaging applications. *Packaging Technology and Science: An International Journal*, 19(1), 1–24. <https://doi.org/10.1002/pts.704>
- Platzer, M., Kiese, S., Tybussek, T., Herfellner, T., Schneider, F., Schweiggert-Weisz, U., & Eisner, P. (2022). Radical scavenging mechanisms of phenolic compounds: A quantitative structure-property relationship (QSPR) study. *Frontiers in Nutrition*, 9, Article 882458. <https://doi.org/10.3389/fnut.2022.882458>
- Qi, W., Qi, W., Xiong, D., & Long, M. (2022). Quercetin: its antioxidant mechanism, antibacterial properties and potential application in prevention and control of toxipathy. *Molecules*, 27(19), 6545. <https://doi.org/10.3390/molecules27196545>
- Regulation 10/2011. *Commission Regulation (EU) No 10/2011 of 14 January 2011 on plastic materials and articles intended to come into contact with food.* (<https://eurlex.europa.eu/legalcontent/EN/TXT/?uri=CELEX%3A32011R0010&qid=1684428637411>).
- Regulation 2016/1416. *Commission Regulation (EU) 2016/1416 of 24 August 2016 amending and correcting Regulation (EU) No 10/2011 on plastic materials and articles intended to come into contact with food (Text with EEA relevance)* OJ L 230, 25.8.2016, p. 22–42. (<https://eur-lex.europa.eu/eli/reg/2016/1416/oj/eng>).
- Rojas, A., Velasquez, E., Pina, C., Galotto, M. J., & de Dicastillo, C. L. (2021). Designing active mats based on cellulose acetate/polycaprolactone core/shell structures with different release kinetics. *Carbohydrate polymers*, 261, Article 117849. <https://doi.org/10.1016/j.carbpol.2021.117849>
- Rossi, V., Cleeve-Edwards, N., Lundquist, L., Schenker, U., Dubois, C., Humbert, S., & Joliet, O. (2015). Life cycle assessment of end-of-life options for two biodegradable packaging materials: Sound application of the European waste hierarchy. *Journal of Cleaner Production*, 86, 132–145. <https://doi.org/10.1016/j.jclepro.2014.08.049>
- Prior, R. L., & Schaich, K. (2005). Standardized methods for the determination of antioxidant capacity and phenolics in foods and dietary supplements. *Journal of Agricultural and Food Chemistry*, 53, 4290–4302. <https://doi.org/10.1021/jf0502698>
- Shen, M., Song, B., Zeng, G., Zhang, Y., Huang, W., Wen, X., & Tang, W. (2020). Are biodegradable plastics a promising solution to solve the global plastic pollution? *Environmental Pollution*, 263, Article 114469. <https://doi.org/10.1016/j.envpol.2020.114469>
- Soroudi, A., & Jakubowicz, I. (2013). Recycling of bioplastics, their blends and biocomposites: A review. *European Polymer Journal*, 49(10), 2839–2858. <https://doi.org/10.1016/j.eurpolymj.2013.07.025>
- Thakur, M., Majid, I., Hussain, S., & Nanda, V. (2021). Poly (ϵ -caprolactone): A potential polymer for biodegradable food packaging applications. *Packaging Technology and Science*, 34(8), 449–461. <https://doi.org/10.1002/pts.2572>
- Velásquez, E., Rojas, A., Pina, C., Galotto, M. J., & López de Dicastillo, C. (2019). Development of bilayer biodegradable composites containing cellulose nanocrystals with antioxidant properties. *Polymers*, 11(12), 1945. <https://doi.org/10.3390/polym11121945>
- Vidal, C. P., Velásquez, E., Galotto, M. J., & de Dicastillo, C. L. (2022). Development of an antibacterial coaxial bionanocomposite based on electrospun core/shell fibers loaded with ethyl lauroyl arginate and cellulose nanocrystals for active food packaging. *Food Packaging and Shelf Life*, 31, Article 100802. <https://doi.org/10.1016/j.fpsl.2021.100802>
- Wachirahuttapong, S., Thongpin, C., & Sombatsompop, N. (2016). Effect of PCL and compatibility contents on the morphology, crystallization and mechanical properties of PLA/PCL blends. *Energy Procedia*, 89, 198–206. <https://doi.org/10.1016/j.egypro.2016.05.026>
- Yang, D., Wang, T., Long, M., & Li, P. (2020). Quercetin: Its main pharmacological activity and potential application in clinical medicine. *Oxidative Medicine and Cellular Longevity*, 2020(1), Article 8825387. <https://doi.org/10.1155/2020/8825387>
- Zhang, C., Lan, Q., Zhai, T., Luo, J., & Yan, W. (2018). Melt crystallization behavior and crystalline morphology of polylactide/poly(ϵ -caprolactone) blends compatibilized by lactide-caprolactone copolymer. *Polymers*, 10, 1181. <https://doi.org/10.3390/polym10111181>
- Zeng, Y., Song, J., Zhang, M., Wang, H., Zhang, Y., & Suo, H. (2020). Comparison of in vitro and in vivo antioxidant activities of six flavonoids with similar structures. *Antioxidants*, 9(8), 732. <https://doi.org/10.3390/antiox9080732>